LILRA5 functions to induce ROS production on innate immune cells

Zuyi Fu[1], Matevž Rumpret[1], Irina Kube-Golovin[2], Mykola Lyndin[2,3], Vera Solntceva[1], Yuxi Zhao[4], Anastasiia Konieva[2], Na Liu[5], Adrian T. Press[5,6,7], Stefanie B. Flohé[8], Michael Bauer[5,6], Gunther Wennemuth[2], Bernhard B. Singer[2] & Alex J. McCarthy[1*]

Affiliations:

[1]Centre for Bacterial Resistance Biology, Section of Molecular Microbiology, Department of Infectious Diseases, Imperial College London, London, SW7 2AZ, UK.

[2]Department of Anatomy, Medical Faculty, University of Duisburg-Essen, Essen, 45147, Germany.

[3]Academic and Research Medical Institute, Department of Pathology, Sumy State University, 40000, Sumy, Ukraine.

[4]Department of Medical Microbiology, UMC Utrecht, Utrecht, 3584 CX, The Netherlands.

[5]Jena University Hospital, Department of Anesthesiology and Intensive Care Medicine, 07747 Jena, Germany.

[6]Jena University Hospital, Center for Sepsis Control and Care, Bachstr. 12, 07743 Jena, Germany.

[7]Friedrich-Schiller-University, Medical Faculty, 07747 Jena, Germany.

[8]University Hospital Essen, Department of Trauma Surgery, 45147 Essen, Germany

***Corresponding author:**

Centre for Bacterial Resistance Biology, Section of Molecular Microbiology, Department of Infectious Diseases, Imperial College London, London, SW7 2AZ, UK.

a.mccarthy@imperial.ac.uk.

Author email addresses:

Z.F. = z.fu@imperial.ac.uk

M.R. = m.rumpret@imperial.ac.uk

I.K.-G. = irina.kube-golovin@uk-essen.de

M.K. = n.lyndin@med.sumdu.edu.ua

V.S. = vera.solntceva@icr.ac.uk

Y.Z. = y.zhao1@lumc.nl

A.K. = a.konieva@med.sumdu.edu.ua

N.L. = na.liu@med.uni-jena.de

A.T.P = adrian.press@med.uni-jena.de

S.B.F = stefanie.flohe@uk-essen.de

M.B = michael.bauer@med.uni-jena.de

G.W. = gunther.wennemuth@uk-essen.de

B.B.S = deceased

A.J.M. = a.mccarthy@imperial.ac.uk

Keywords: Activating Receptor, Reactive Oxygen Species, LILRA5, Infection, Sepsis

Abbreviations:

DAMP Damage-associated molecular pattern

52 **DB** Dynabeads

53 **FcαR** Fc alpha receptor

54 **FcRγ** Fc receptor gamma-chain

55 **FCS** Foetal calf serum

56 **FITC** Fluorescein Isothiocyanate

57 **GFP** Green fluorescent protein

58 **IFN-γ** Interferon gamma

59 **IgG1** Immunoglobulin G1

60 **IL-1β** Interleukin-1 beta

61 **IL-6** Interleukin 6

62 **ITAM** Immunoreceptor tyrosine-based activation motif

63 **LAIR1** Leukocyte associated immunoglobulin–like receptor 1

64 **LILRA2** Leukocyte Immunoglobulin like receptor A2

65 **LILRA5** Leukocyte Immunoglobulin like receptor A5

66 **LPS** Lipopolysaccharide

67 **mAb** Monoclonal antibody

68 **NFAT** Nuclear factor of activated T cells

69 **PAMP** Pathogen-associated molecular pattern

70 **PBMCs** Peripheral blood mononuclear cells

71 **PE** Phycoerythrin

72 **ROS** Reactive oxygen species

73 **TNF-α** Tumour necrosis factor alpha

Abstract (200 words)

Activating immune receptors provide mechanisms for phagocytes to elicit important effector functions that promote the killing of microbes. Leukocyte immunoglobulin-like receptor A5 (LILRA5) an orphan immune receptor expressed by human phagocytes and co-localising with FcRγ, remains poorly characterised. To address this, we developed a highly-specific anti-LILRA5 monoclonal antibody that has agonistic properties. Using a specific anti-LILRA5 antibody, we show LILRA5 expression on naïve monocytes and neutrophils, and that ligation of LILRA5 stimulates ROS production. While increased *LILRA5* transcript copy numbers have been associated with sepsis, we also observed increased levels in patients with systemic infection but without sepsis complications. *Ex vivo* bacterial infection of whole blood did not alter surface LILRA5 expression, but LPS stimulation changed expression levels. This indicates that surface LILRA5 expression is dynamic and likely regulated post-transcriptionally, changing responses to different stimuli or over time. Soluble (s)LILRA5 was enhanced in sera from sepsis patients and in supernatants of monocytes that were LPS-stimulated, indicative that shedding of LILRA5 from cell surfaces or that expression of sLILRA5 isoforms provides a mechanism to regulate surface LILRA5 expression levels. Finally, we show that altered surface LILRA5 expression influences LILRA5-induced ROS production capacity. We propose that LILRA5 is a dynamically regulated activating receptor expressed on phagocytes that can stimulate ROS production.

Introduction

Phagocytic immune cells such as neutrophils, monocytes and macrophages play a key role in the innate immune response to infection (1). They can kill invading pathogens by engulfing them through phagocytosis, releasing antimicrobial molecules and generating reactive oxygen species (ROS). The capacity of these immune cells to respond to stimuli in the environment is attributed to the expression of immune receptors on the cell surface that detect signs of infection. Given the importance of phagocytosis, degranulation and ROS generation, these processes can be activated via several innate immune receptors. This includes receptors containing immunoreceptor tyrosine-based activation motif (ITAM) in the cytoplasmic tail (2–4), or those that co-associate with the ITAM-containing FcRγ (1,5). Though several innate immune receptors co-associate with FcRγ (6), their capacity to activate phagocytes, induce degranulation and/or stimulate ROS production is less well understood.

Leukocyte immunoglobulin-like receptor A5 (LILRA5, ILT11, LIR9, CD85f) is a type I transmembrane receptor and member of the leukocyte immunoglobulin-like receptor (LILR) family (7). *LILRA5* transcripts are expressed by neutrophils, monocytes and macrophages (8,9). Though surface LILRA5 expression has been reported for monocytes and macrophages (8), the expression of LILRA5 on neutrophil surfaces remains unclear (10). Structurally, LILRA5 contains an extracellular region formed of two immunoglobulin (Ig) domains, a transmembrane region that contains a positively charged arginine residue for co-localisation with the ITAM-containing FcRγ and a short cytoplasmic tail (8). It can also be expressed in a soluble form known as sLILRA5 (8,9). Though the ligands of LILRA5 are unknown (7,11), cross-linking LILRA5 on monocyte surfaces induces association with FcRγ, phosphorylation of the ITAMs in FcRγ, increased activation of the Src and Syk kinases and release of pro-inflammatory cytokines (8). Mice with deletion of the *LILRA5* gene displayed an increased susceptibility to bacterial keratitis and a dysregulated inflammatory response (12).

120 Due to the scarcity of highly-specific anti-LILRA5 mAbs and no knowledge on endogenous
121 and exogenous LILRA5 ligands (10), the expression and functions of LILRA5 are poorly
122 elucidated. Recent reports have shown that *LILRA5* transcripts are significantly increased in
123 human bacterial keratitis and in human sepsis (12,13). This is suggestive that LILRA5 has a
124 role in bacterial defence and could be a useful biomarker for rapid diagnosis of inflammation
125 triggered by bacterial pathogens. In this study, we developed a highly-specific antibody against
126 LILRA5 as a tool to investigate expression and functions. We investigated *LILRA5* transcript
127 levels and surface LILRA5 expression on phagocytes in health and disease, and assessed
128 whether cross-linking LILRA5 could trigger ROS production and phagocytosis.

129 Results

130 Development of LILRA5-specific mAb with agonistic properties

131 To analyse the expression of LILRA5 on human immune cells, we developed a mouse
132 monoclonal antibody that specifically recognised LILRA5. To do this, recombinant (r)LILRA5
133 was expressed in a eukaryotic expression system and purified (**Fig. 1A**). Anti-LILRA5 P4-11A
134 mAb was purified from a hybridoma derived from fusion of myeloma NS1/0 cells with spleen
135 cells from Balb/c mice immunised with rLILRA5-His. We characterised the specificity of the
136 mAb for LILRA5 by testing its binding to Dynabeads (DB) coated with rLILR-His or rLAIR1-His
137 (**Supp. Fig. 1A**). Flow cytometry analysis revealed that anti-LILRA5 P4-11A mAb binds to
138 human rLILRA5, but to not any of the closely related human rLILR that are most likely to be
139 cross-reactive, nor to an immune receptor from a different family called LAIR1 (**Fig. 1B, Supp.
140 Fig. 1B**). The isotype matched IgG did not bind to rLILRA5. Furthermore, anti-LILRA5 P4-11A
141 mAb is bound to rLILRA5-coated DB in a concentration-dependent manner (**Supp. Fig. 1C**).
142 This data suggests that anti-LILRA5 P4-11A mAb has high-specificity for detecting LILRA5.
143 We next investigated the capacity of anti-LILRA5 P4-11A mAb to bind LILRA5 presented at
144 the cell surface. Firstly, we generated a LILRA5+ U937 cell line by transducing the parental

145 U937 cell line with a lentiviral vector encoding the coding domain sequence of *LILRA5* and
146 selecting transductants. We then tested the binding of anti-LILRA5 P4-11A mAb to wildtype
147 U937 and LILRA5+ U937 cell lines. Flow cytometry analysis revealed enhanced binding of
148 anti-LILRA5 P4-11A mAb to the LILRA5+ U937 cells compared to control U937 cells (**Fig. 1C**),
149 revealing anti-LILRA5 mAb P4-11A can specifically detect cell surface expressed LILRA5.
150
151 As cross-linking is crucial for studying mAb-induced LILRA5 function, we tested whether anti-
152 LILRA5 P4-11A mAb could cross-link and activate LILRA5 in a reporter cell model. We
153 generated 2B4T NFAT-GFP reporter cells that express the LILRA5CD3ζ fusion protein at the
154 cell surface (**Fig. 1D**). The engagement of CD3ζ in the control 2B4T NFAT-GFP cells and the
155 LILRA5CD3ζ-expressing 2B4T NFAT-GFP induced GFP expression (**Supp. Fig. 2A**). Plate-
156 bound rabbit polyclonal anti-LILRA5 antibodies induced the expression of GFP in
157 LILRA5CD3ζ-expressing, but not control, 2B4T NFAT-GFP cells (**Supp. Fig. 2B**). This
158 confirmed that cross-linking LILRA5CD3ζ chimaera induces GFP expression. Plate-bound
159 anti-LILRA5 P4-11A mAb induced the expression of GFP in LILRA5CD3ζ-expressing, but not
160 control, 2B4T NFAT-GFP cells (**Fig. 1E**). In contrast, incubation of either cell on plate-bound
161 isotype IgG1 did not induce GFP expression. Therefore, anti-LILRA5 P4-11A mAb has
162 agonistic properties for LILRA5 that can be utilised as a molecular tool to study LILRA5
163 signalling and functions.
164
165 Since soluble LILRA5 (sLILRA5) can be expressed by human immune cells (8,9), we
166 investigated if anti-LILRA5 P4-11A could be used as a capture antibody in an ELISA assay.
167 We used rLILRA5-His as a standard and rabbit anti-LILRA5 polyclonal antibodies for
168 detection. The ELISA detected rLILRA5-His, but not rLAIR1-His as a control protein, in a
169 concentration-dependent manner **(Fig. 1F)**. Based on these results, we conclude that the anti-
170 LILRA5 P4-11A antibody only binds to human LILRA5, does not cross-react with other LILRs
171 and has cross-linking capacity.

172 **LILRA5 is expressed on the surface of human neutrophils and monocytes**

173 The expression of *LILRA5* transcripts has been detected in primary human neutrophils and
174 monocytes from healthy donors (9), but LILRA5 protein levels on neutrophils was never
175 reported (10). We revisited the issue of transcript and protein expression, by analysing
176 contemporary RNA-seq data from two independent studies and by using the anti-LILRA5 P4-
177 11A mAb to detect protein expression with high-specificity. Analysis of RNA-seq data showed
178 that *LILRA5* transcript abundance was comparable between neutrophils and monocyte
179 populations, but at a lower level on dendritic cells (DCs) (**Fig. 2A**). These results indicate that
180 human monocytes and human neutrophils express *LILRA5* transcripts at comparable levels.
181 The binding of PE-conjugated anti-LILRA5 P4-11A to the surface of primary immune cells from
182 n = 3 healthy donors detected expression of LILRA5 on the surface 95.58 ± 7.44 % of
183 monocytes and 99.57 ± 0.47 % of neutrophils (**Fig. 2B** and **Supp. Fig. 3**). Analysis of the
184 binding of anti-LILRA5 P4-11A to the surface of purified monocytes (anti-LILRA5 5.28 ± 3.05
185 vs. IgG1 1.17 ± 0.25) (**Fig. 2C** and **2D**) and purified neutrophils (anti-LILRA5 1.55 ± 0.26 vs.
186 IgG1 1.24 ± 0.19) (**Fig. 2C** and **2E**) confirmed that both cell types express LILRA5. Notably,
187 the surface LILRA5 expression was lower for neutrophils when compared to monocytes.
188 Taken together, this reveals that naïve neutrophils and monocytes express comparable
189 transcript levels of *LILRA5*, while monocytes express higher protein levels of LILRA5 on their
190 cell surfaces.
191

192 **Respiratory burst can be stimulated through LILRA5**

193 Next, we investigated whether LILRA5 cross-linking via anti-LILRA5 P4-11A could induce
194 respiratory burst in neutrophils and monocytes. In these assays, we incubated human
195 neutrophils or PBMCs in the presence of plate-bound anti-LILRA5 P4-11A mAb or isotype
196 IgG1 control. We used anti-CD89 mAb as a positive control as it induces ROS production by
197 cross-linking FcαR (CD89) and inducing a signal through FcRγ (14,15). Incubation of PBMCs

198 from healthy donors with plate-bound anti-CD89 mAb or anti-LILRA5 P4-11A mAb, but not
199 isotype IgG1 control, resulted in the ROS production (**Fig. 3A** and **3B**). As LILRA5 and FcαRI
200 are not expressed on lymphocytes, ROS production is most likely elicited through the
201 monocyte population in the PBMCs. Of note, LILRA5-induced ROS production was almost as
202 potent as FcαR-induced ROS production. Likewise, neutrophils from healthy donors produced
203 ROS in response to plate-bound anti-CD89 mAb and anti-LILRA5 P4-11A mAb, but not isotype
204 IgG1 control (**Fig. 3C** and **3D**). This data indicates that LILRA5 can induce respiratory bursts
205 in human monocytes and neutrophils.

206 ***LILRA5* transcripts are elevated in systemic infection and sepsis**

207 It was recently reported that *LILRA5* expression in monocytes is a biomarker of sepsis, a life-
208 threatening organ dysfunction that occurs when the immune system overreacts to an infection
209 (13,16). Therefore, we investigated the expression properties of *LILRA5* transcripts and
210 LILRA5 protein in sepsis patients. We first assessed whether enhanced *LILRA5* expression
211 was increased in whole blood of sepsis patients compared to healthy controls in additional
212 datasets that were not analysed in previous studies. The elevated *LILRA5* expression in whole
213 blood in sepsis patients was evident in several independent datasets **(Fig 4A** and **Supp Fig.**
214 **4A, 4B** and **4C)**. As previous analysis revealed that monocytes display enhanced *LILRA5*
215 transcripts during sepsis (13,16), we questioned whether neutrophils as well as monocytes
216 also display enhanced *LILRA5* expression in sepsis patients. We addressed this by analysing
217 the Demaret *et al.* dataset (17), which revealed that *LILRA5* expression was enhanced in
218 neutrophils purified from the peripheral blood of sepsis patients compared to healthy controls
219 **(Fig. 4B).** Expression of *LILRA5* transcripts was also elevated in monocytes from sepsis
220 patients compared to healthy controls in a previously unanalysed dataset **(Fig. 4C)**. Thus,
221 *LILRA5* expression is increased in whole blood, neutrophils and monocytes during human
222 sepsis.
223

224 To understand whether enhanced *LILRA5* expression is a marker of sepsis *per se*, it is
225 important to establish whether patients with bacterial and viral infections that have not
226 progressed to sepsis display modified *LILRA5* expression. First, we analysed the whole blood
227 transcript dataset of Dix *et al.* from patients with diagnosed bacterial infections and controls
228 (18). Here, *LILRA5* expression was increased in the whole blood of patients upon hospital
229 presentation that were subsequently diagnosed with a *S. aureus* or *E. coli* invasive infection
230 compared to healthy controls **(Supp Fig. 4D)**. Next, we analysed whole blood transcriptome
231 data from healthy individuals, febrile children with confirmed bacterial infections and febrile
232 children with confirmed viral infections from the Herberg *et al.* (19). This revealed that *LILRA5*
233 expression is enhanced in individuals with bacterial infection or viral infection compared to
234 healthy controls **(Supp Fig. 4E).** Finally, we analysed the dataset from Herwanto *et al.* to
235 compare *LILRA5* expression in whole blood of healthy individuals, patients with diagnosed but
236 uncomplicated infections (based on a sequential organ failure assessment (SOFA) score on
237 admission (≥ 2 vs. < 2), in accordance with the international consensus definition of sepsis
238 ("sepsis-3")), patients with sepsis and patients that progressed to septic shock (20). In this
239 dataset, *LILRA5* transcripts in whole blood were significantly increased in patients with
240 diagnosed but uncomplicated infections, in sepsis patients and in septic shock patients
241 compared to healthy controls **(Fig. 4D)**. In sum, *LILRA5* expression is not significantly different
242 between sepsis patients and patients with diagnosed but uncomplicated infections, suggestive
243 that elevated *LILRA5* expression in whole blood is not a marker of sepsis *per se*.

244 Surface LILRA5 expression does not increase upon immune challenge

245 Given the elevated *LILRA5* transcripts in whole blood during infectious and inflammatory
246 diseases, we hypothesised that the expression of surface LILRA5 would be increased on
247 immune cells under these conditions. A previous transcriptome analysis revealed that 4 hours
248 of *ex vivo* infection of human blood with *E. coli*, but not *S. aureus,* induced a significant
249 increase in expression of *LILRA5* **(Fig. 5A).** We assessed the binding of anti-LILRA5 P4-11A
250 mAb to monocytes purified from human whole blood that had been infected with *E. coli* or *S.*

251 *aureus*. Surprisingly, surface LILRA5 expression was not differentially regulated on monocytes
252 after *ex vivo* infection with *E. coli* or with *S. aureus* **(Fig. 5B)**. Collectively, these results suggest
253 that bacterial challenges induce elevated *LILRA5* expression in monocytes, but no altered
254 surface LILRA5 expression on monocytes.
255
256 To ascertain whether our *ex vivo* findings were representative of *in vivo* immune challenge,
257 we examined the binding of anti-LILRA5 P4-11A mAb to PBMCs purified from sepsis patients
258 and healthy controls. The sepsis patients had confirmed infections with Gram-negative
259 bacteria (*n* = 12; 46 %), Gram-positive bacteria (*n* = 6; 23 %) or Candida (*n* = 3; 12 %), or
260 unidentified aetiology (*n* = 4; 15 %). We specifically measured the LILRA5-signal on
261 monocytes by co-staining the PBMCs with APC-conjugated anti-CD14, PE-conjugated HLA-
262 DR and FITC-conjugated anti-LILRA5. Notably, there was no significant difference in surface
263 LILRA5 expression levels on monocytes from sepsis patients at day 1 of diagnosis compared
264 to healthy controls **(Fig. 5C)**. Furthermore, the surface LILRA5 expression on monocytes
265 remained largely unchanged during the progression of sepsis in individual patients **(Fig. 5D)**.
266 Therefore, *LILRA5* transcripts expression in innate immune cells is enhanced during immune
267 challenge, but the surface LILRA5 expression remains unchanged.

268 **Soluble LILRA5 is elevated in serum from sepsis patients**

269 Given our previous observations we queried how *LILRA5* transcripts could increase upon
270 systemic infection and inflammation, but surface LILRA5 expression levels remained
271 unchanged. As *LILRA5* can undergo alternative mRNA splicing to generate transcripts that
272 encodes two different sLILRA5 isoforms (9), a switch in mRNA splicing could explain our
273 previous results. Alternatively, our results could arise if there was no switch in mRNA splicing
274 but surface LILRA5 was shed from cell surfaces. Under either scenario, it would be expected
275 that sLILRA5 levels are elevated under immune challenge. To test this, we compared sLILRA5
276 in serum from sepsis patients and healthy donors using the ELISA assay and anti-LILRA5 P4-
277 11A. The mean signal for sLILRA5 in serum from 128 patients with clinical defined sepsis was

278 significantly higher than in serum from 60 healthy controls **(Fig. 5E)**. Taken together, this
279 suggests that immune challenge increases sLILRA5 levels, indicative of splice changes or cell
280 shedding.

281 **Immune challenge impacts LILRA5-induced ROS production**

282 To investigate the functional consequences of altered *LILRA5* transcripts or surface LILRA5
283 expression, we challenged PBMCs with the potent immune stimulator LPS. LPS induces a
284 significant increase in *LILRA5* transcript expression in monocytes **(Fig. 6A)**, and lead to a
285 trend (p = 0.0683) for increased surface LILRA5 expression **(Fig. 6B)**. Since there was an
286 increased surface LILRA5 expression on monocytes during LPS stimulation, we assessed the
287 impact of this dynamic change on cellular function. As in our previous experiments, we
288 measured the capacity of anti-LILRA5 P4-11A to induce ROS production when cells were pre-
289 stimulated with LPS. Surprisingly, there was a significant reduction in LILRA5-dependent ROS
290 production for cells that had been stimulated with LPS compared to untreated cells (**Fig. 6C**
291 and **6D**). This indicates that LPS challenge increases *LILRA5* transcripts and expression of
292 surface and soluble LILRA5, but that LILRA5 is less effective at inducing respiratory burst.

293 ## Discussion

294 Here, we demonstrate that human phagocytes express surface LILRA5 and that it promotes
295 important effector functions of respiratory burst and degranulation. We show that LILRA5 is
296 expressed on the surface of both circulating neutrophils and monocytes in healthy donors.
297 Since oxidative burst is induced by immune receptors that act to sense non-self and that signal
298 through ITAMs (21), our data imply that LILRA5 has a role in mounting innate immune
299 responses. Enhanced ROS production, mediated through a LILRA5-dependent mechanism
300 during infection or immune challenge, would contribute to the killing of microbes within the
301 phagolysosome following successful phagocytosis. Indeed, deletion of LILRA5 in mice led to
302 enhanced progression of *P. aeruginosa*-induced inflammation and keratitis (12). Additionally,
303 the increased release of antimicrobial factors, such as proteases and peptides, into the local
304 environment following LILRA5-triggered exocytosis of granules, would further promote
305 microbial killing.

306

307 The level of activating receptor expression on an immune cell is an important determinant of
308 its capacity to induce cellular activation. Notably, a substantially higher expression of surface
309 LILRA5 expression is present on circulating monocytes compared to neutrophils in healthy
310 individuals, even though there is a comparable level of *LILRA5* transcripts. This differential
311 expression suggests that LILRA5 may have distinct roles on monocytes and neutrophils.
312 Interestingly, even with the lower surface expression of LILRA5 on neutrophils, our assays
313 demonstrate that ROS production can still be effectively induced via LILRA5 cross-linking.
314 This indicates that LILRA5, although less abundant on neutrophils, is functionally competent
315 and capable of triggering significant immune responses. The higher expression of LILRA5 on
316 the surface of monocytes might reflect a more prominent role in sustained immune activation
317 and regulation, whereas the presence on neutrophils, albeit at lower levels, underscores its
318 importance in rapid, acute responses to infection

319

320 The immune system initiates a swift immune response to detect non-self in order to protect
321 the host. The upregulation of *LILRA5* expression at transcript levels in whole blood, monocytes
322 and neutrophils in response to infection or immune challenge, suggests that it has a role in
323 sensing or mounting responses against microbes and/or non-self. In line, it has previously
324 been reported that expression of mRNA encoding membrane-anchored LILRA5 in monocytes
325 is dynamic and increases upon exposure to cytokines (8). Given this, we hypothesised that
326 the increased *LILRA5* expression upon immune challenge would be correlated with an
327 increase in surface LILRA5 expression on immune cells. Surprisingly, our study revealed that
328 surface LILRA5 expression does not change on the surface of monocytes during infection of
329 bacterial pathogens *ex vivo*. Additionally, monocytes from sepsis patients displayed no change
330 in surface LILRA5 expression compared to healthy controls. This could be explained if the
331 increased *LILRA5* transcripts encode sLILRA5 but not membrane-bound LILRA5. *sLILRA5*
332 expression is reported in multiple immune cell types and varies between individuals (22). In
333 line, sLILRA5 was detected in sera of sepsis patients in our study, and in the synovial fluid of
334 rheumatoid arthritis patients and in sera of patients with liver steatosis (8,23). Our studies did
335 identify a trend for increased expression of surface LILRA5 on monocytes after their
336 stimulation with LPS. These results suggest that surface LILRA5 expression is dynamic,
337 changing in response to different stimuli and/or over time. Further investigation is needed to
338 elucidate the precise mechanisms governing both surface and soluble LILRA5 expression and
339 their functional implications in immune responses.
340
341 The function of an activating receptor is dependent on the sensing of a ligand, but LILRA5 has
342 no defined ligand (7,10,11). Most activating receptors on phagocytes sense PAMPs, DAMPs,
343 antibody-opsonised microbes or complement-opsonised microbes (21,24). However, LILRA2,
344 a receptor in the same family, can sense microbially-cleaved antibodies to trigger antibacterial
345 effector functions (25). This raises the prospect that LILRA5 could also sense infection by
346 detecting modified self ligands. sLILRA5 may act to regulate membrane-anchored LILRA5

347 functions by competing for the same ligand. Thus, the identification of LILRA5 ligands is
348 important to understand its biological and evolutionary properties.
349
350 Enhanced *LILRA5* expression in whole blood or monocytes has been reported as a sepsis
351 biomarker in patient cohorts (12,13). However, *LILRA5* transcripts are also increased in
352 patients with diagnosed bloodstream infections. Furthermore, *LILRA5* transcript levels in
353 whole blood do not significantly differ between patients with diagnosed but uncomplicated
354 infection and patients with sepsis. Since levels of *LILRA5* transcripts cannot differentiate these
355 two patient groups, this suggests that *LILRA5* is not a biomarker of sepsis *per se*. Our analysis
356 of sLILRA5 in serum revealed elevated levels in sepsis patients compared to healthy controls.
357 Additional quantitative studies are required to test the robustness of this finding, and to
358 ascertain whether quantifying sLILRA5 in sera is a putative biomarker of sepsis.
359
360 In conclusion, this study was underpinned by the development of a novel LILRA5-targeting
361 mAb, anti-LILRA5 clone P4-11A, that detects LILRA5 with high specificity and possesses
362 agonistic properties. LILRA5 is expressed by human phagocytes and promotes ROS
363 production. Immune challenge can induce dynamic increases in *LILRA5* transcript levels, but
364 unchanged or increased surface LILRA5 expression. This regulates LILRA5-dependent ROS
365 production. Future studies are required to identify LILRA5 ligands and to further elucidate the
366 regulatory mechanisms and functions of membrane-bound LILRA5 and sLILRA5.

367 # Materials & Methods

368 ## Ethical Approval

369 Human blood was obtained from healthy donors, approved by the Regional Ethics Committee
370 and Imperial College Healthcare NHS Trust Tissue Bank (Regional Ethics Committee approval
371 no. 17/WA/0161, Imperial College Healthcare Tissue Bank Human Tissue Authority licence
372 no. 12275, and Imperial College Research Ethics Committee no. 19IC5166). The study was
373 approved by the local ethics committee of the Friedrich-Schiller- University Jena for samples
374 from sepsis patients (ID:2019-1306_2-Material) and healthy donors (ID:2022-2847-Material).
375 All samples were collected after receiving signed informed consent from all participants.
376 Serum sepsis samples were approved by the Ethics Committee of Sumy State University
377 (protocol number 12, approval date December 11th 2021).

378 ## Expression and purification of rLILR-His

379 EXPI293F cells were cultured in EXPI media at 37°C with 5% CO_2, as previously described
380 (15,26). The expression of rLILRB1-His, rLILRB3-His and rLILRA6-His have been previously
381 described (15). To construct expression vectors for LILRA5, the remaining LILR and LAIR-1,
382 the signal peptide and extracellular domains of LILRs were amplified from cDNA vectors
383 (**Table 1**) and inserted into pcDNA3.4 vectors. The forward primers contained a pcDNA3.4
384 backbone overhang, a *Bam*HI restriction site, Kozak sequence and a gene-specific region.
385 The reverse primers contained pcDNA3.4 backbone, a *Not*I restriction site, a stop codon, a
386 6xHis tag and a gene-specific region. PCR amplification was performed using Phusion High-
387 Fidelity Taq Polymerase (Thermo Fisher Scientific) and thermocycling as follows: 1 cycle
388 (98°C for 2 min), 35 cycles (98°C 15 s, 62°C 30 s, and 72°C 30 s), and 1 cycle (72°C 10 min).
389 Recombinant His-tagged proteins were purified from culture supernatants by affinity
390 chromatography (ÄKTA pure; GE Healthcare Life Sciences) using HIStrap nickel columns (GE

391 Healthcare Life Sciences), and elutions were dialysed into 50 mM Tris 300 mM NaCl (pH 8)
392 and stored at -80°C.

393 **Generation of anti-LILRA5 mAb**

394 Generation of LILRA5-specific mAb was performed using the hybridoma technique of Köhler
395 and Milstein (27). A Balb/c mouse was immunised with rLILRA5-His (David's Biotechnologie,
396 Germany). Spleen cells from Balb/c mice were recovered and fused to myeloma NS1/0 cells.
397 The soluble IgG expressed by individual hybridoma clones were tested for binding rLILRA5-
398 His by ELISA allowing the identification of clone P4-11A. The mAb was produced in a serum-
399 and azide-free medium to ensure purity and minimise potential contaminants.

400 **Binding of mAb to Dynabeads or cells**

401 Dynabeads His-Tag Isolation and Pulldown (Thermo Fisher Scientific) were incubated with C-
402 terminal His-tagged rLILR or rLAIR-1 proteins following manufacturer protocols to generated
403 coated-DBs. DBs were incubated with 5 µg/ml of mAb in buffer (PBS + 0.5% BSA for DB) for
404 30 mins at 4°C. After washing, DB were incubated with 50 µl of PE-conjugated goat anti-
405 mouse IgG secondary antibody (1:300; Invitrogen) under the same conditions. The
406 fluorescence of DBs was measured by flow cytometry and analysed based on the FSC and
407 SSC parameters.
408

409 **Leukocyte immunophenotyping by flow cytometry**

410 Hetasep (STEMCELL Technologies, Vancouver, Canada) was diluted in whole blood (1:7 v/v)
411 and incubated for 30 min at room temperature. The supernatant was collected and washed
412 with culture medium (RPMI1640 with stable glutamine (Bio&Sell, Feucht, Germany), 100 U/ml
413 Penicillin, 100 µg/ml Streptomycin (both Gibco/ThermoFisher, Waltham, Massachusetts))
414 supplemented with 2% FCS (Biochrom; v/v). Platelets were removed by centrifugation at 200
415 g for 10 min without brake. Residual red blood cells were lysed with Red Blood Cell Lysis
416 Solution (Miltenyi Biotec, Bergisch Gladbach, Germany) according to the manufacturer's

417 instructions. Isolated leukocytes were incubated with human TruStain FcX (Biolegend, San
418 Diego, CA, USA) and stained with 10 µg anti-CD14-APC (Immunotools, Friesoythe,
419 Germany), anti-CEACAM8 (clone 6/40c), and anti-LILRA5-11A (in house labeled with PE)
420 each. Staining with the corresponding isotype control antibodies (mIgG-FITC, mIgG-PE,
421 mIgG-APC; Immunotools, Friesoythe, Germany) was performed to determine the threshold
422 for specific staining. Data were acquired using MACSQuant® Analyzer 10 (Miltenyi Biotec,
423 Bergisch Gladbach, Germany) and analysed using MACSQuantify™ Software 2.13 (Miltenyi
424 Biotec, Bergisch Gladbach, Germany). Monocytes were gated as CD14+ cells and neutrophils
425 as CEACAM8+ cells. The median fluorescence intensity (MFI) of LILRA5 or isotype control
426 was determined. Individual expression of LILRA5 was calculated as [MFI LILRA5 - MFI Isotype
427 control].

428 **Isolation of primary human neutrophils and PBMCs**

429 Neutrophils and PBMCs were isolated from whole blood by Ficoll/Histopaque centrifugation
430 and resuspended in RPMI1640 supplemented with 5% FCS, as previously described (15).
431 Neutrophils were isolated with >98% purity and 99% viability.

432 **Binding of mAb to cells or primary immune cells**

433 45 µl of 5 x 10^6 cells/ml of cell lines or purified primary immune cells were incubated with 5
434 µg/ml of mAb in buffer (PBS + 0.5% BSA for DB, or RPMI1640 supplemented with 10% FCS
435 for cells) for 30 min at 4°C. After washing, cells were incubated with 50 µl of PE-conjugated
436 goat anti-mouse IgG secondary antibody (1:300; Invitrogen) under the same conditions. The
437 fluorescence of cell lines or purified primary immune cells was measured by flow cytometry
438 and analysed based on the FSC and SSC parameters.

439 **ELISA for detection of sLILRA5**

440 Wells of 96-well plates were coated overnight with 50 µl of 2 µg/ml anti-LILRA5 clone P4-11A
441 mAb in PBS at 4°C. After washing (3 times with PBS + 0.05% Tween-20), wells were blocked

442 with 100 µl PBS + 5% BSA for an hour at room temperature. After three washes with PBS +
443 0.05% Tween-20, wells were incubated with 100 µl of rLILRA5-His or rLAIR1-His (at varying
444 concentrations) in buffer or heat-inactivated human serum samples for 1 hour at 4°C. After
445 washing (3 times with PBS + 0.05% Tween-20), 50 µl of rabbit anti-LILRA5 pAb (1:2000; Sino
446 Biological) was added to the wells and incubated as above. For the detection of the rabbit anti-
447 LILRA5 pAb, wells were incubated with 50 µl of horseradish peroxidase (HRP)-conjugated
448 goat anti-rabbit-IgG antibody (1:10,000; A16096; Life Technologies) under the same condition.
449 After washing (3 times with PBS + 0.05% Tween-20), the assay was developed with 100µl
450 1xTMB substrate and 100µl Stop solution for TMB substrate (Invitrogen).

451 **Generation of LILRA5-expressing U937 cell line**

452 U937 cell lines were cultured in RPMI1640 supplemented with 10% FCS and
453 penicillin/streptomycin at 37°C with 5% CO_2. To construct a LILRA5-expressing U937 cell line,
454 a DNA fragment containing the coding domain sequence of LILRA5 was amplified from a
455 LILRA5 cDNA vector (HG16059-G, BioConnect) using primers
456 $^{5'}$GAGCTAGCAGTATTAATTAACCACCATGGCACCATGGTCTCATCCATC$^{3'}$ and
457 $^{5'}$GTACCGGTTAGGATGCATGCTCACCTTCCAGCTGCAGCTTGGG$^{3'}$. PCR amplification
458 was performed using Phusion High-Fidelity Taq Polymerase (Thermo Fisher Scientific) and
459 thermocycling as follows: 1 cycle (98°C for 2 min), 35 cycles (98°C 15 s, 60°C 30 s, and 72°C
460 30 s), and 1 cycle (72°C 10 min). The purified amplicon was ligated into a dual promoter
461 lentiviral vector (BIC-PGK-Zeo-T2a-mAmetrine; RP172 derived from
462 no.2025.pCCLsin.PPT.pA.CTE.4‑-scrT.eGFP.mCMV.hPGK.NG-FR.pre, as previously
463 described (15) via Gibson reaction using a parental vector digested with *Pac*I and *Sph*I.
464 Lentiviral particles were created in HEK293T cells and transfected into U937 cells, as

465 previously described (15,28). Transfected cells were selected by culture in media
466 supplemented with 400 µg/mL zeocin.

467 **Generation of LILRA5CD3ζ reporter cell line and GFP induction**

468 2B4 NFAT-GFP T cell reporter cells contain an NFAT-GFP fusion construct containing three
469 tandem NFAT-binding sites fused to enhanced GFP cDNA (28). 2B4 T cell lines were cultured
470 in RPMI1640 supplemented with 10% FCS and pen/strep at 37ºC with 5% CO_2. A
471 LILRA5CD3ζ reporter cell line was generated, as previously described (15). In brief, a DNA
472 fragment containing the coding domain sequence of the LILRA5 extracellular and
473 transmembrane domains and the CD3ζ cytoplasmic tail was synthesised by Integrated DNA
474 Technologies. The fragment was ligated into the RP172 vector, as described above. After
475 selection and expansion, the resultant cell cultures were tested for LILRA5 expression using
476 anti-LILRA5 pAb (16059-RP01; Sino Biological) and flow cytometry analysis. To induce GFP
477 expression, TC-treated 96-well plates were coated at 4°C overnight with 40 µl of 5 µg/ml
478 Hamster anti-CD3ζ clone 145-2C11 (BD Biosciences), anti-LILRA5 pAb (16059-RP01; Sino
479 Biological), anti-LILRA5 P4-11A mAb, or IgG isotype control mAbs diluted in PBS. After
480 washing, 96-well plates were seeded with two hundred microliters of 2B4T cells at a density
481 of 2.5×10^5 cells/ml in RPMI 1640 containing 10% FCS, 100 µg/ml penicillin, and 100 µg/ml
482 streptomycin. After centrifugation at 200 rpm for 3 mins, cells were cultured at 37°C with 5%
483 CO_2 for 18 hours. The cells were then resuspended in PBS and fluorescence was measured
484 by flow cytometry analysis.

485 **Reactive oxygen species (ROS) production upon LILRA5 cross-linking**

486 To quantify ROS production, wells of a white 96-well plate was coated overnight at 4°C with
487 50 µl of 5 µg/ml anti-LILRA5 clone P4-11A mAb, anti-CD89 (MCA1824; Bio Rad) or IgG1
488 Isotype control (0102-01; Southern Biotech) mAbs diluted in $NaHCO_3$ buffer, pH8.6. The plate
489 was then washed twice with PBS. Neutrophils and PBMCs were washed with ice-cold reaction

490 buffer (20 mM HEPES, 140 mM NaCl, 1 mM $CaCl_2$, 5 mM Glucose, pH7.4) three times and
491 resuspended to 1 x 10^6 cells/ml. To each well, 100 µl of 1 x 10^6 cells and 100 µl of pre-warmed
492 reaction buffer containing 20 mM Amplex Red (Life Technologies) were added. For the assays
493 performed with PBMCs, the reaction buffer was additionally supplemented with 10 µl of
494 horseradish peroxidase (1 unit/ml; P8125-5KU; Sigma Aldrich). Fluorescence was measured
495 by a CLARIOstar microplate reader with detection at 2-min intervals for 2 hours at 37°C. Area
496 under the curve (AUC) for each stimulus was calculated after subtraction of background/PBS
497 ROS production. In specific experiments, cells were stimulated with 5 µg/ml LPS from
498 *Escherichia coli* O111:B4 (Sigma–Aldrich) for one hour at 37°C with 5% CO_2.

499 **Activation of neutrophils and monocytes by LILRA5 cross-linking and/or LPS**

500 Wells of a white 96-well plate were coated overnight at 4°C with 50 µl of 5 µg/ml anti-LILRA5
501 clone P4-11A mAb or IgG1 Isotype control (0102-01; Southern Biotech) mAbs diluted in PBS.
502 The plate was then washed twice with PBS. Neutrophils and PBMCs were resuspended to 1
503 x 10^6 cells/ml in a solution made up of 80% of RPMI 1640 + penicillin/streptomycin and 20%
504 of plasma from the same donor. To each well, 200 µl of 1 x 10^6 cells/ml was added and cultured
505 for 24 hours at 37°C with 5% CO_2. In certain assays, neutrophils and PBMCs were stimulated
506 with 1 µg/ml or 10 ng/ml LPS from *Escherichia coli* O111:B4 (Sigma–Aldrich) for 24 hours at
507 37°C with 5% CO_2, respectively. Wells coated without antibodies and/or without LPS were
508 used as a control. Neutrophils were collected and stained with anti-CD66b-FITC (1:50; BD
509 Biosciences) for 30 mins at 4°C. In parallel, PBMCs were stained with 3µg/ml anti-CD14-FITC
510 (367116, Biolegend) under the same conditions. After washing, the fluorescence of cells was
511 measured by flow cytometry and analysed based on the forward- and side-scatter plots.

512 ***LILRA5* expression profiling in transcriptome studies**

513 The expression of *LILRA5* was assessed in retrieved data from previous array profiling data
514 available on the Gene Expression Omnibus (GEO–NCBI) using GEO2R (NCBI). Datasets

515 analysed were as follows:- 1) to assess *LILRA5* expression in whole blood of sepsis patients
516 and controls = GSE134364 from (29), GSE137342 from Mukhopadhyay, GSE185263 from
517 (30), 2) to assess *LILRA5* expression in neutrophils purified from sepsis patients and controls
518 = GSE64457 from (17), 3) to assess *LILRA5* expression in monocytes purified from sepsis
519 patients and controls = GSE180387 from (31), 4) to assess *LILRA5* expression in whole blood
520 of sepsis patients, septic shock patients, patients with diagnosed but uncomplicated infections
521 and controls GSE154918 from (20), 5) to assess *LILRA5* expression in whole blood of patients
522 with diagnosed bacterial or viral infections = GSE72810 from (19) and GSE33341 from (32),
523 6) to assess LILRA5 expression in whole blood after ex vivo infection with *E. coli* or *S. aureus*
524 = GSE65088 from (18), 7) to assess LILRA5 expression in monocytes after culture for 18
525 hours ± LPS = GSE147310 from (33)

526 **LPS-stimulation of leukocytes and quantification of surface LILRA5 and sLILRA5**

527 Hetasep (STEMCELL Technologies, Vancouver, Canada) was diluted in whole blood (1:7 v/v)
528 and incubated for 30 min at room temperature. The supernatant was collected and washed
529 with culture medium (RPMI1640 with stable glutamine (Bio&Sell, Feucht, Germany), 100 U/ml
530 Penicillin, 100 µg/ml Streptomycin (both Gibco/ThermoFisher, Waltham, Massachusetts))
531 supplemented with 2% FCS (Biochrom; v/v). Platelets were removed by centrifugation at 200
532 g for 10 min without brake. Residual red blood cells were lysed with Red Blood Cell Lysis
533 Solution (Miltenyi Biotec, Bergisch Gladbach) according to the manufacturer's instructions.
534 Cultures were set up in culture medium supplemented with 4% FCS at $4x10^5$ cells/well/200 µl
535 in 96-well ultra-low attachment culture plates (Corning, New York #3474) at 37°C with 5%
536 CO_2. After 60 min, cells were stimulated with 50 ng/ml *E.coli* 026:B6 LPS (Sigma, St. Louis,
537 Missouri) for further 18 h. Leukocytes were incubated with human TruStain FcX (Biolegend,
538 San Diego, CA) and stained with anti-CD14-APC (Immunotools, Friesoythe), anti-HLADR-PE
539 (Invitrogen/ ThermoFisher Waltham, Massachusetts), and anti-LILRA5-11A (in house labeled
540 with FITC) as described previously (34). Staining with the corresponding isotype control

541 antibodies was performed to determine the threshold for specific staining. The threshold was
542 set at 3% false positive cells. Data were acquired using CytoFLEX S (Beckman Coulter,
543 Krefeld, Germany) and analysed using CytExpert (Beckman Coulter). Monocytes were gated
544 as CD14+HLA-DR+ cells and the median fluorescence intensity (MFI) of LILRA5 or isotype
545 control was determined. Individual expression of LILRA5 was calculated as [MFI LILRA5 - MFI
546 Isotype control].

547 **Whole blood infection and measurement of surface LILRA5 expression on monocytes**

548 To stimulate whole blood, 1 x 10^7 CFU of *E. coli* MG1655 or *S. aureus* JE2 were inoculated
549 into 10 mL of whole blood for a 2-hour incubation at 37°C. PBMCs were then isolated using
550 the standard protocol described previously. Cells (45 µL of 5 x 10^6 cells/mL) were incubated
551 with 3 µg/mL IgG1 Isotype control (0102-01; Southern Biotech) or anti-LILRA5 P4-11A mAb
552 in RPMI 1640 supplemented with 10% FCS for 30 minutes at 4°C. After washing with 1x PBS,
553 cells were incubated with 50 µL of PE-conjugated goat anti-mouse IgG secondary antibody
554 (1:300; Invitrogen) under the same conditions. The fluorescence of cells was measured by
555 flow cytometry and analysed based on the forward- and side-scatter plots.

556 **Analysis of monocytes and serum from sepsis patients**

557 Sepsis was diagnosed according to the Sepsis-3 criteria (35). In total, *n* = 26 patients (16
558 males and 10 females) with sepsis were enrolled at the Department of Anesthesiology and
559 Intensive Care Medicine, University Hospital Jena, Germany. The median (IQ range) age of
560 the patients was 65 (53-72). The source of infection was Gram-negative bacteria (*n* =12; 46
561 %), Gram-positive bacteria (*n* = 6; 23 %), Candida (*n* = 3; 12 %), or unidentified (4; 15 %).
562 Heparinised blood was drawn within 24 h after admission to the intensive care unit (ICU). If
563 the patient remained on the ICU blood was collected up to two more times on day 7 and day
564 14 after admission. Whole blood from healthy donors (*n* = 9) with median age (IQ range) 52
565 (30-57) was used as control. The study was approved by the local ethic committee of the
566 Friedrich-Schiller University Jena for samples from patients (ID:2019-1306_2-Material) and

567 healthy donors (ID:2022-2847-Material) and of the University Hospital Essen (for samples
568 from healthy donors). Informed consent was obtained from each patient or the respective legal
569 representative and from healthy donors.

570

571

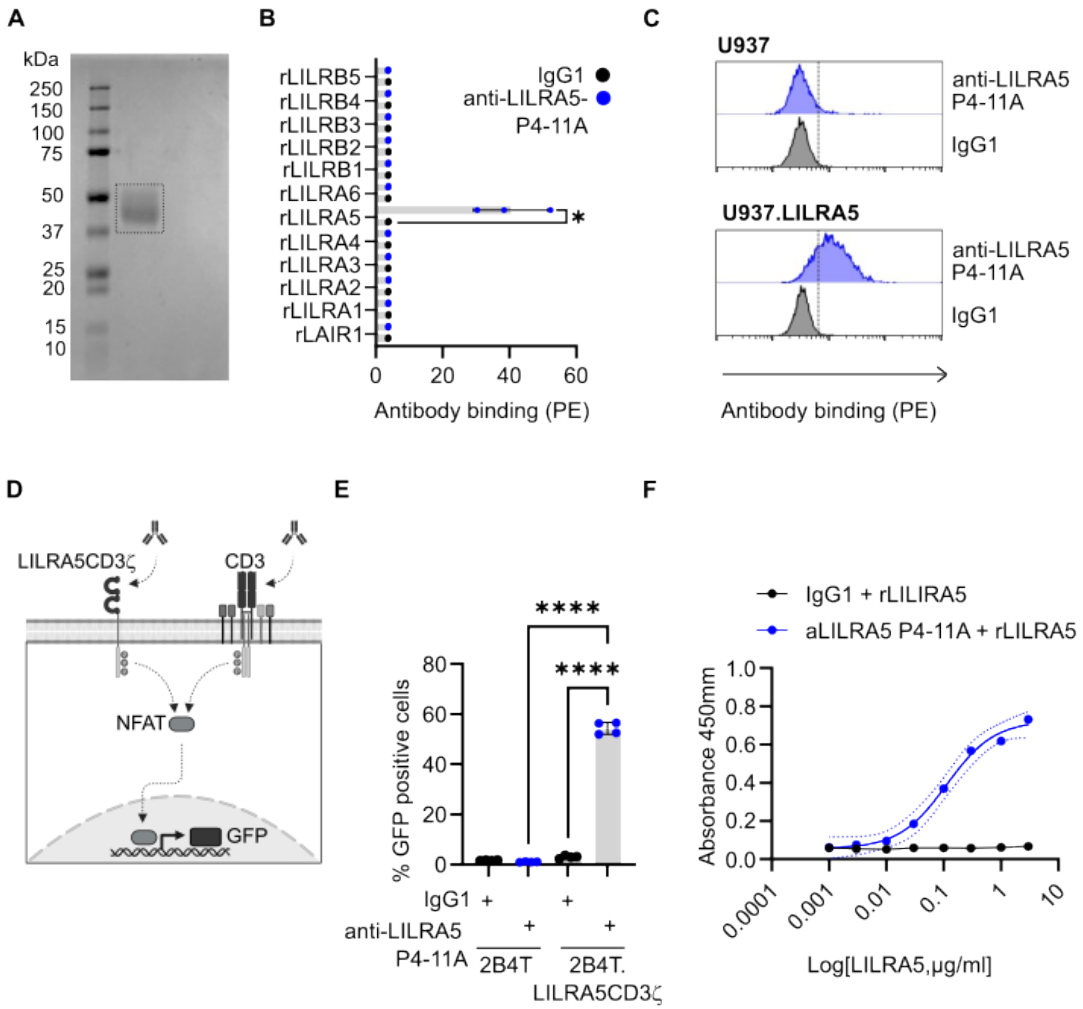

572

573

574 **Figure 1: A highly specific anti-LILRA5 antibody with cross-linking capacity (A)** SDS-
575 PAGE analysis of rLILRA5-His, used for immunisation of Balc/c mice. **(B)** Binding of anti-
576 LILRA5 P4-11A mAb to magnetic beads coated with recombinant LILR or control proteins.
577 mAb binding was detected using anti-IgG mAb and flow cytometric analysis. Mean ± SD of *n*
578 = 3 independent experiments is shown. Paired *t*-test between anti-LILRA5 P4-11A and isotype
579 control, where $*p < 0.05$. **(C)** U937 cells transfected with DNA vectors expressing LILRA5
580 protein, or control cells, were analysed for binding of anti-LILRA5 clone P4-11A mAb. mAb
581 binding was detected using anti-IgG mAb and flow cytometric analysis. *n* = 3 from 3
582 independent experiments, one representative experiment is shown. **(D)** A schematic of the

583 LILRA5CD3ζ reporter 2B4 T cell line, expressing a surface protein composed of extracellular
584 and transmembrane LILRA5 domains fused to the cytoplasmic tail of CD3ζ. The cross-linking
585 of CD3 or the fusion LILRA5CD3ζ protein induces phosphorylation of the ITAM
586 (immunoreceptor tyrosine-based activation motif) domains in CD3ζ by Src kinases, and a
587 signalling cascade that activates the NFAT (nuclear factor of activated T-cells) transcription
588 factor. NFAT subsequently induces the expression of green fluorescent protein (GFP). **(E)**
589 Cross-linking capacity of plate-bound anti-LILRA5 P4-11A mAb assessed using a
590 LILRA5CD3ζ reporter cell line. GFP expression by LILRA5CD3ζ+ 2B4T cells or control 2B4T
591 cells was assessed by flow cytometric analysis after incubation in wells containing plate-bound
592 anti-LILRA5 P4-11A or isotype mAb. The % of GFP+ cells were quantified. Mean ± SD of n =
593 4 independent experiments are shown. One-way ANOVA, where ****$p < 0.0001$. **(F)**
594 Development of an ELISA for detecting sLILRA5. anti-LILRA5 P4-11A mAb or isotype control
595 were used to capture rLILRA5-His. A titration curve ($n = 3$) of rLILRA5-His detected by anti-
596 LILRA5 P4-11A mAb is shown.

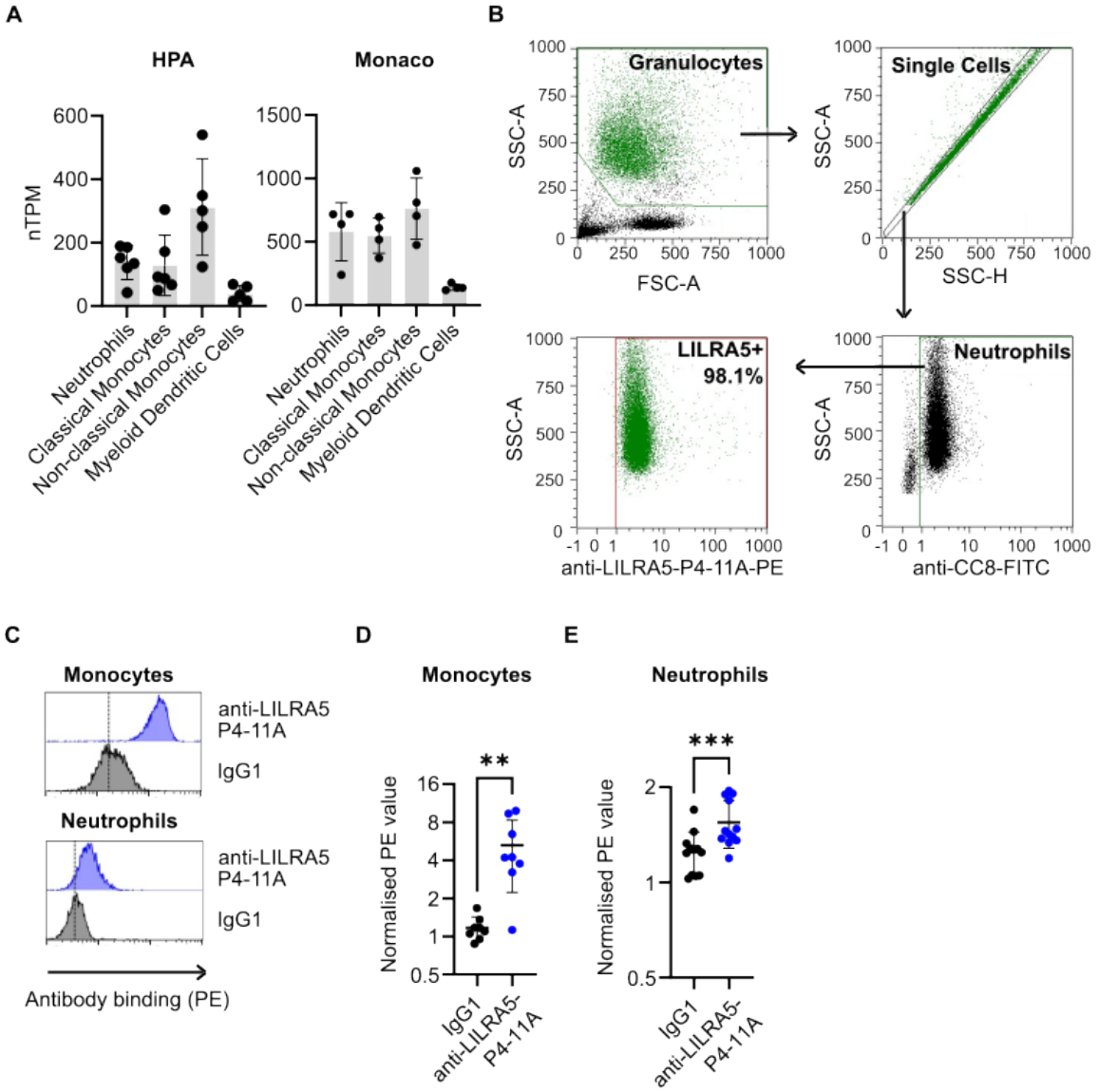

Figure 2: LILRA5 is expressed on human phagocytes. (A) The normalised transcripts per million (nTPM) from the HPA dataset and the Monaco dataset are shown. nTPM values give a quantification of the transcript abundance which is comparable across samples and genes. nTPM values for classical monocytes that have been characterised to express LILRA5 is shown as a control. Mean ± SD are shown. **(B)** Representative example showing the gating strategy used to identify granulocyres in human whole blood using anti-CEACAM8 (CC8; clone 6/40c) and anti-LILRA5 (clone P4-11A). A first gate was set on physical parameters of SSC-A vs. FSC-A, then on SSC-A and SSC-H to eliminate doublets, then granulocytes and

608 monocytes were gated on CD14+ and CEACAM8+, then on CEACAM8+ events to identify
609 granulocytes. **(C, D** and **E)** Expression of LILRA5 on human monocytes and neutrophils
610 analysed by flow cytometry analysis. C shows a representative FACS staining indicating
611 LILRA5 expression in neutrophils and monocytes from a healthy donor. D and E show
612 quantification of the geometric mean of monocytes (n = 8 independent donors) and neutrophils
613 (n = 12 independent donors) stained with anti-LILRA5 clone P4-11A or isotype control,
614 respectively. Paired t-test, where $^{**}p < 0.01$ and $^{***}p < 0.001$.

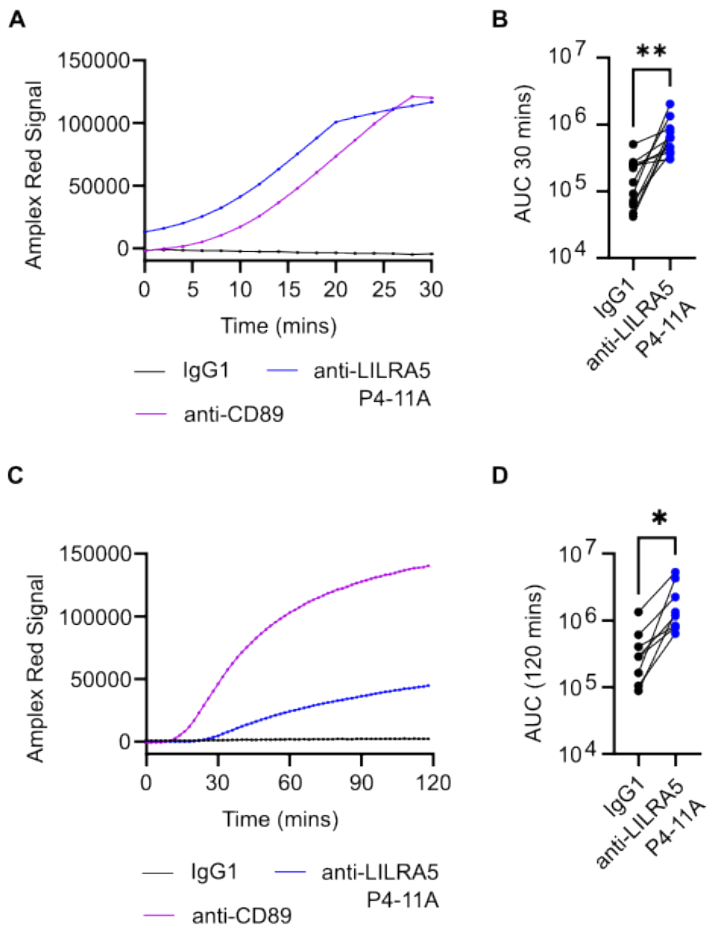

615

616 **Figure 3: LILRA5 stimulates ROS production and in human phagocytes. (A** and **B)**
617 Stimulating LILRA5 on PBMCs induces reactive oxygen species (ROS) production, as
618 measured using Amplex Red. A representative plot is shown in A. Mean ± SD of n = 7
619 independent donors is shown in B. A paired-sample t-test was used to compare Area Under
620 the Curve (AUC) after stimulating PBMCs with anti-LILRA5 P4-11A or isotype IgG1 control,
621 where *$p < 0.05$. **(C** and **D)** Stimulating LILRA5 on neutrophils induces ROS production, as
622 measured using Amplex Red. A representative plot is shown in C. Mean ± SD of n = 8
623 independent donors is shown in D. A paired-sample t-test was used to compare AUC after
624 stimulating neutrophils with anti-LILRA5 P4-11A or isotype IgG1 control, where *$p < 0.05$.

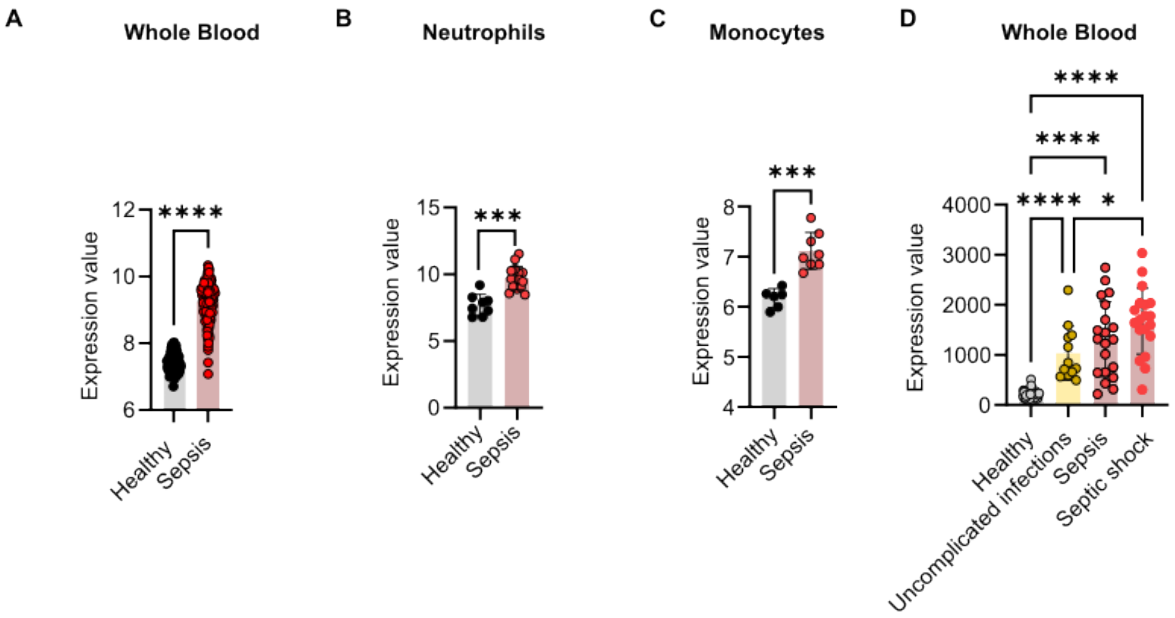

Figure 4: *LILRA5* expression in sepsis patients. (A) *LILRA5* expression in whole blood of healthy donors (n = 83) or sepsis patients (n = 156) (GSE134364). Mean ± SD are shown. Statistics tested by *limma*, where adjusted ***p < 0.001. **(B)** *LILRA5* expression on neutrophils from healthy donors (n = 8) or sepsis patients (n = 15) (GSE64457). Mean ± SD are shown. Statistics tested by *limma*, where adjusted ***p < 0.001. **(C)** *LILRA5* expression in CD14+ monocytes from healthy donors (n = 6) or sepsis patients (n = 8) (GSE180387). Mean ± SD are shown. Statistics tested by *limma*, where adjusted ***p < 0.001. **(D)** *LILRA5* expression in whole blood of healthy donors (n = 40), patients with diagnosed but uncomplicated systemic infection (n = 12), sepsis patients (n = 20) or septic shock patients (n = 19) (GSE154918). Mean ± SD are shown. Statistics tested by *limma*, where adjusted ***p < 0.001.

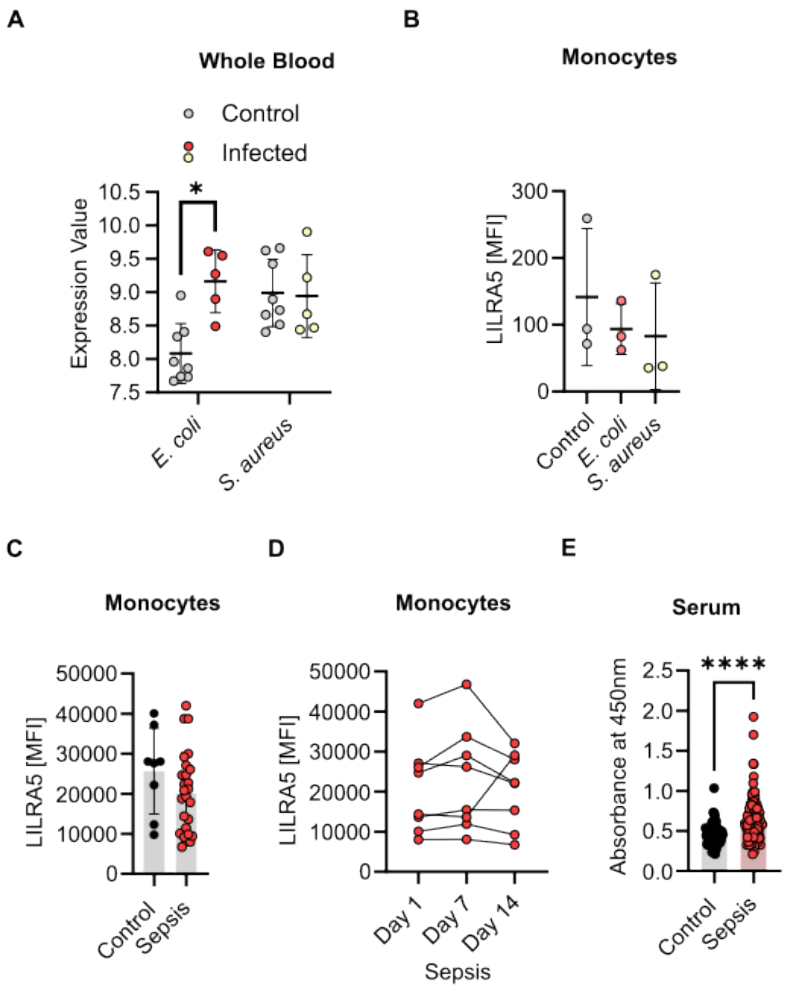

Figure 5: Surface LILRA5 expression does not increase during infection and inflammation. (A) *LILRA5* expression in whole blood from healthy donors after 4-hour *ex vivo* infection with *E. coli* (n = 5, control n = 8) or *S. aureus* (n = 5, control n = 8) (GSE65088). Mean ± SD are shown. Statistics tested by *limma* adjusted ***$p < 0.001$. **(B)** Expression of LILRA5 on human monocytes after *ex vivo* infection of whole blood by *E. coli* or *S. aureus*, analysed by flow cytometry analysis. One-way ANOVA was used to compare the mean fluorescence intensity (MFI) from anti-LILRA5 P4-11A staining (after subtracting of MFI isotype IgG1) for infection vs control, where **$p < 0.01$ and *$p < 0.05$, is shown for n = 3 independent donors. **(C)** Surface LILRA5 expression on human monocytes from healthy donors (n = 8) and sepsis patients (n = 26), upon hospital admission, analysed by flow cytometry analysis. Each data point represents the MFI from anti-LILRA5 P4-11A stained cells after subtracting the MFI of isotype IgG1 stained cells. Mean ± SD are shown. **(D)** Surface LILRA5 expression on human

651 monocytes from sepsis patients (*n* = 8) at day 1, day 7 and day 14 of hospital admission,
652 analysed by flow cytometry analysis. Each data point represents the MFI from anti-LILRA5
653 P4-11A stained cells after subtracting the MFI of isotype IgG1 stained cells. **(E)** Comparison
654 of sLILRA5 in serum from sepsis patients (*n* = 128) or healthy donors (*n* = 60). Mean ± SD are
655 shown. Statistics were tested by student t-test, where ****$p < 0.0001$.
656
657
658
659

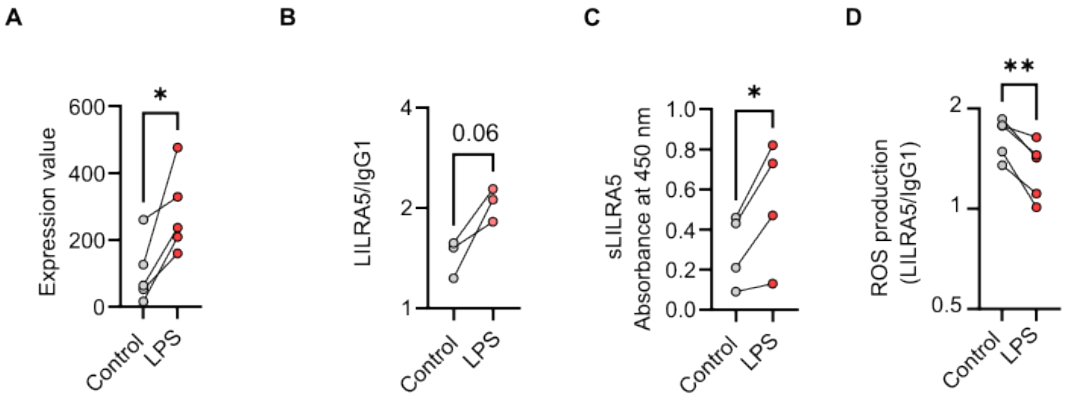

660
661 **Figure 6. LPS activation reduces LILRA5-dependent ROS production. (A)** *LILRA5*
662 expression by monocytes purified from healthy donors that were cultured ± LPS for 18 hours
663 (GSE147310). Data from *n* = 5 donors are shown. Statistics tested by *limma*, where adjusted
664 *$p < 0.05$. **(B)** Surface LILRA5 expression on human monocytes purified from healthy donors
665 (*n* = 3), analysed by flow cytometry analysis. Each data point represents the signal of anti-
666 LILRA5 P4-11A relative to isotype IgG1 control. Statistics tested by paired t-test, where *$p <$
667 0.05. **(C)** sLILRA5 in culture supernatants from PBMCs purified from healthy donors (*n* = 4),
668 after 18 hours culture ± LPS. Statistics were tested by paired t-test, where *$p < 0.05$. **(D)**
669 Production of reactive oxygen species (ROS) by PBMCs in response to LILRA5 ± LPS
670 stimulation, as measured using Amplex Red. ROS production was quantified as the area
671 under the curve (AUC). The ROS production induced by anti-LILRA5 P4-11A relative to IgG1

672 was calculated. Data is shown from $n = 5$ independent donors. Paired *t*-test was relative ROS

673 production induced by anti-LILRA5 P4-11A for control vs LPS-treated cells, where $^{**}p < 0.01$.

674

675

676

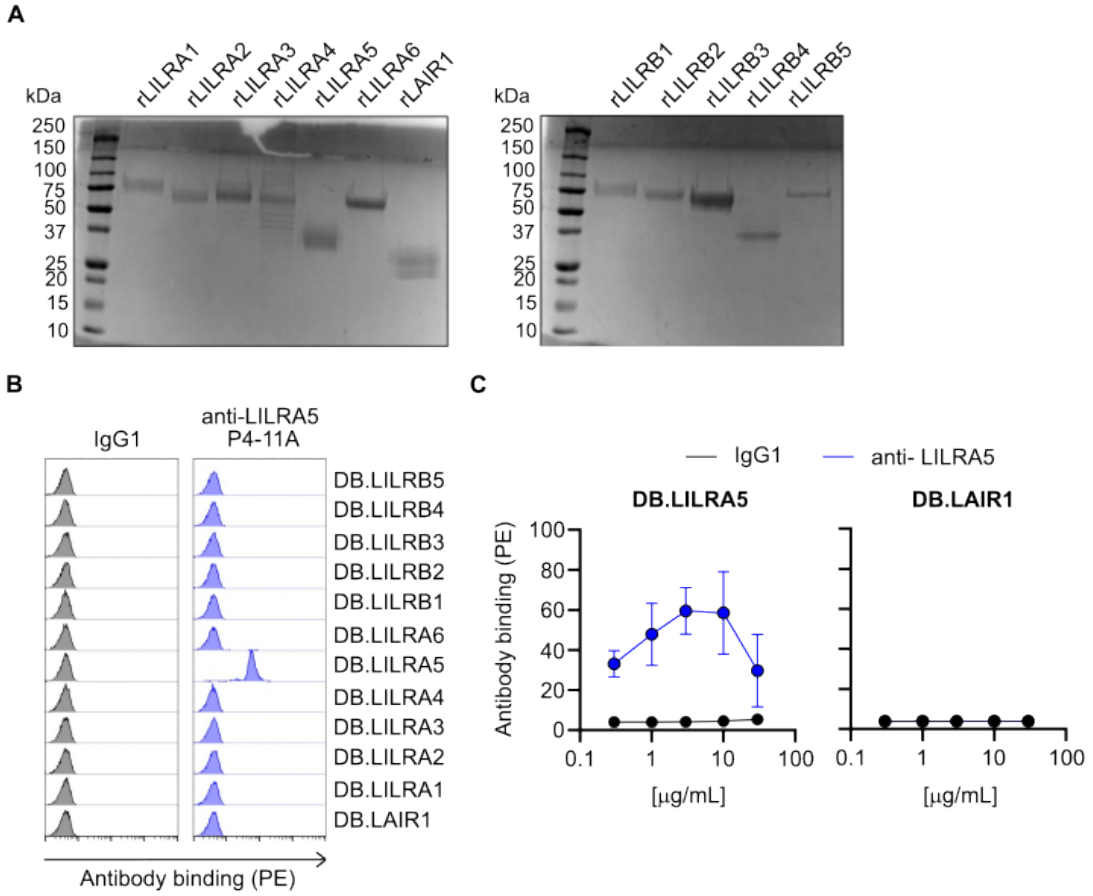

677

678

679 **Supplementary Figure 1: anti-LILRA5 P4-11A mAb binds to LILRA5 with high-**
680 **specificity. (A)** SDS-PAGE analysis of recombinant (r) proteins, used for assessing the
681 specificity of anti-LILRA5 P4-11A mAb. **(B)** Specificity of anti-LILRA5 P4-11A antibody for
682 LILRA5. Magnetic beads coated with rLILR or control proteins and analysed for binding of anti-
683 LILRA5 P4-11A mAb. mAb binding was detected using anti-IgG mAb and flow cytometric
684 analysis. *n* = 3 from 3 independent experiments, one representative experiment is shown. **(C)**
685 Concentration-dependent binding of anti-LILRA5 P4-11A mAb to rLILRA5-coated dynabeads.
686 mAb binding was detected using anti-IgG mAb and flow cytometric analysis. *n* = 3 from 3
687 independent experiments.

688

689

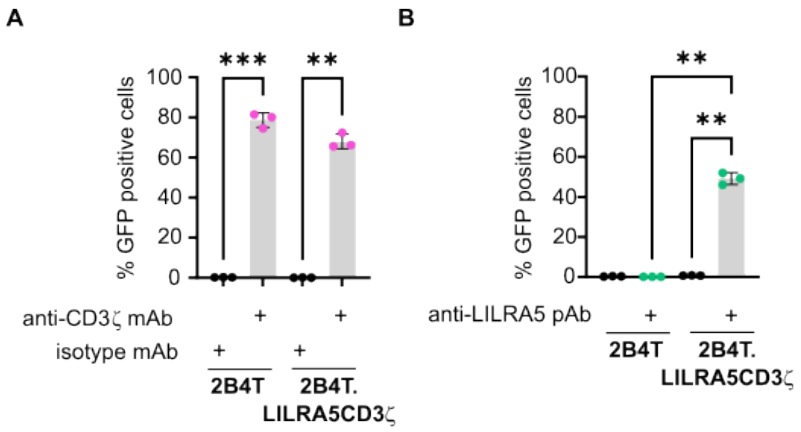

690

691 **Supplementary Figure 2: Validation of LILRA5. (A)** Cross-linking capacity of plate-bound
692 anti-CD3ζ mAb to induce GFP expression in the LILRA5CD3ζ reporter 2B4T cell line and
693 control 2B4T cell line. GFP expression by LILRA5CD3ζ+ 2B4T cells or control 2B4T cells was
694 assessed by flow cytometric analysis after incubation in wells containing plate-bound anti-
695 CD3ζ or isotype mAb. The % of GFP+ cells was quantified. Mean ± SD of n = 3 independent
696 experiments are shown. One-way ANOVA, where ***p < 0.001, **p < 0.01. **(B)** Cross-linking
697 capacity of plate-bound anti-LILRA5 pAb to induce GFP expression in the LILRA5CD3ζ
698 reporter 2B4T cell line and control 2B4T cell line. GFP expression by LILRA5CD3ζ+ 2B4T
699 cells or control 2B4T cells was assessed by flow cytometric analysis after incubation in wells
700 containing plate-bound anti-LILRA5 or buffer control. The % of GFP+ cells were quantified.
701 Mean ± SD of n = 3 independent experiments are shown. One-way ANOVA, where ***p <
702 0.001, **p < 0.01.

703

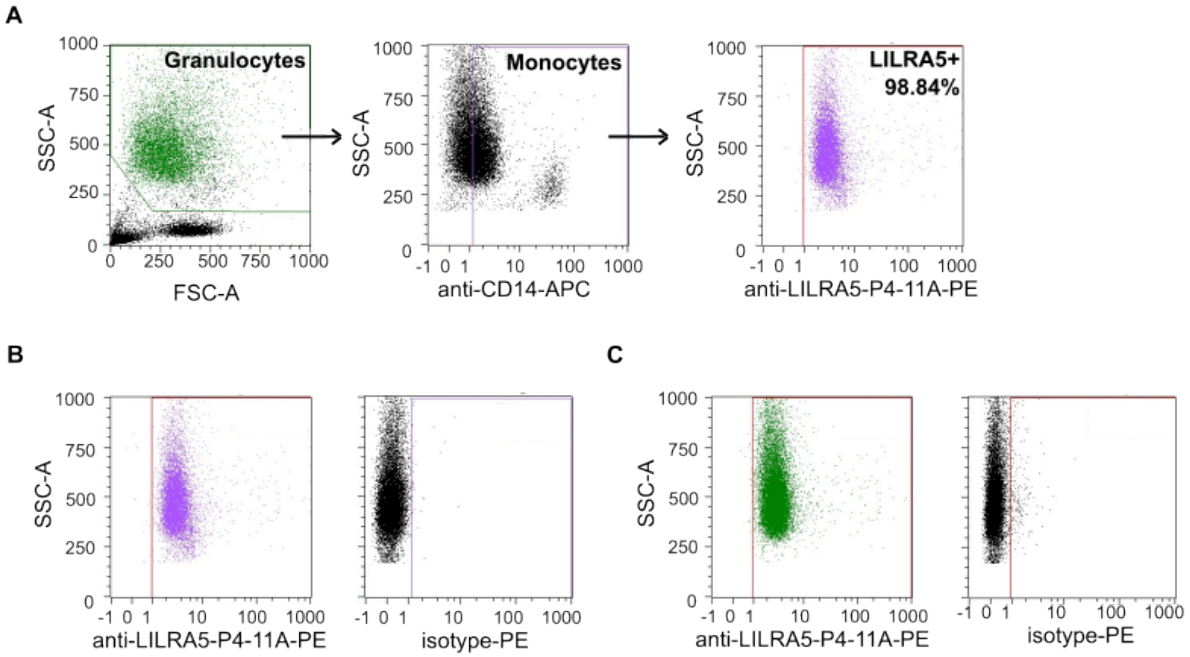

704

705

706 **Supplementary Figure 3: Gating strategy and expression of LILRA5 on monocytes. (A)**
707 Representative example showing the gating strategy used to identify monocytes in human
708 whole blood using anti-CD14 and anti-LILRA5 (clone P4-11A). A first gate was set on physical
709 parameters of SSC-A vs. FSC-A, then on SSC-A and SSC-H to eliminate doublets (not shown,
710 but similarly presented in Fig 2), then monocytes and granulocytes were gated on CD14+ and
711 CEACAM8+ (not shown), then on CD14+ events to identify monocytes. **(B)** Representative
712 flow cytometry histogram showing LILRA5 expression on CD14+ monocytes. **(C)**
713 Representative flow cytometry histogram showing LILRA5 expression on CEACAM8+
714 neutrophils.

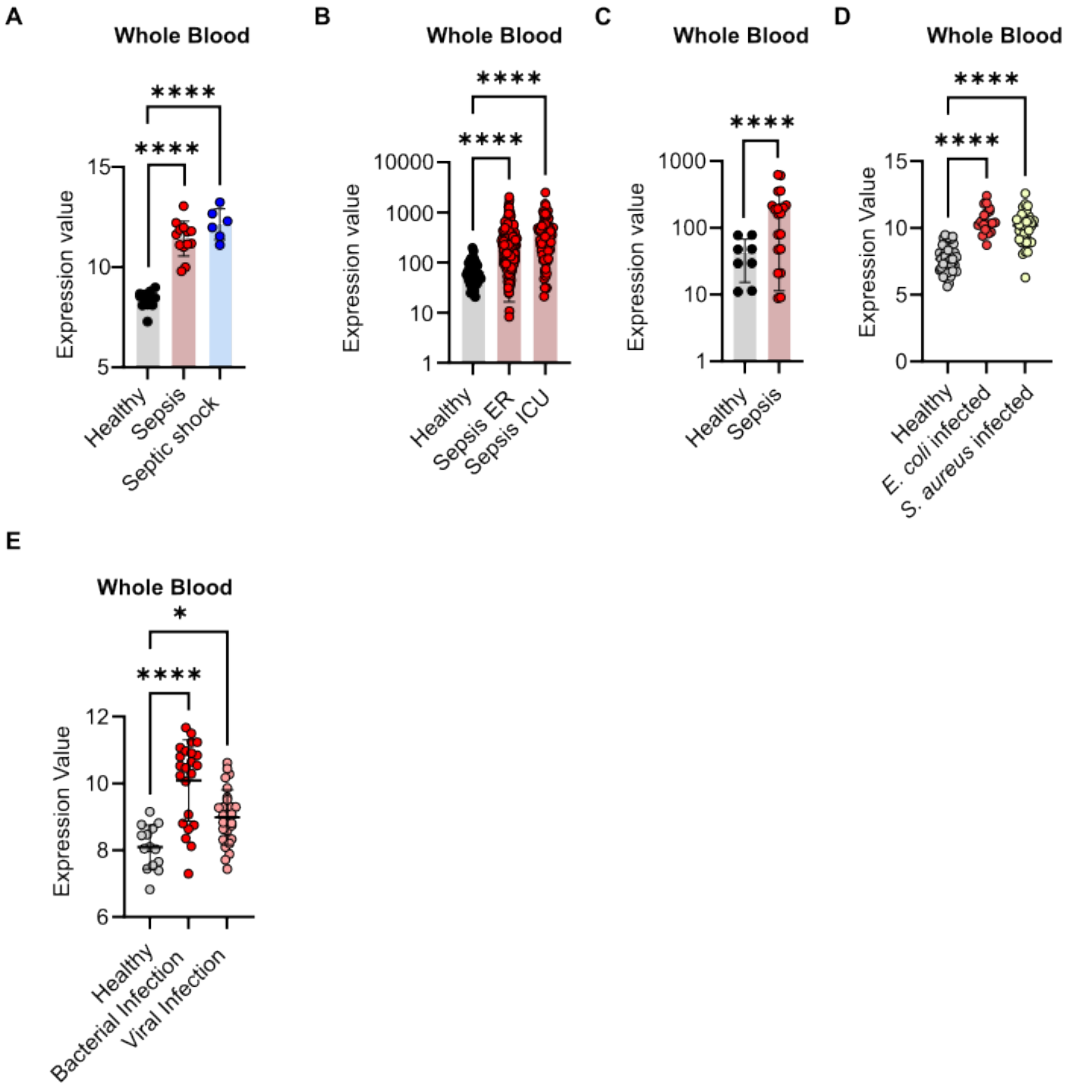

Supp. Fig 4. *LILRA5* expression during sepsis and systemic infection. (A) *LILRA5* expression in whole blood of healthy donors (n = 12) or sepsis patients (n = 13) or septic shock patients (n = 6) (GSE137342). Mean ± SD are shown. Statistics tested by *limma*, where adjusted ***p < 0.001. **(B)** *LILRA5* expression in whole blood of healthy donors (n = 44) or sepsis patients presenting at emergency rooms (ER) (n = 266) or sepsis patients on intensive care units (ICU) (n = 82) (GSE185263). Mean ± SD are shown. Statistics tested by *limma*, where adjusted ***p < 0.001. **(C)** *LILRA5* expression in whole blood of healthy donors (n = 8) or sepsis patients (n = 20) (GSE232753). Mean ± SD are shown. Statistics tested by *limma*, where adjusted ***p < 0.001. **(D)** *LILRA5* expression in whole blood from healthy donors (n =

726 14), patients with bacterial infections (n = 24) and patients with viral infections (n =
727 28)(GSE72810). Mean ± SD are shown. Statistics tested by *limma*, where adjusted ***p <
728 0.001. **(E)** *LILRA5* expression in whole blood from healthy donors (n = 43), patients with *E.*
729 *coli* infection (n = 32), or patients with *S. aureus* infection (n = 19) (GSE33341). Mean ± SD
730 are shown. Statistics tested by *limma*, where adjusted ***p < 0.001.

731 **Table 1: cDNA vectors and amplification primers**

cDNA vector	Primers (5' to 3')
LILRA1 HG17220-G (BioConnect)	Forward: CTCTAGAGGATCGAACCCTTGGATCCACCACCATGACCC CCATCGTCACAGTCCTG Reverse: CTAACCGGTAGGGATCGAACCCTTGCGGCCGCCTAGTGG TGATGGTGGTGATGATTCTCCACTGTGTAATCCTGGGGG
LILRA2 HG13273-G (BioConnect)	Forward: CTCTAGAGGATCGAACCCTTGGATCCACCACCATGACCC CCATCCTCACGGTCCTG Reverse: CTAACCGGTAGGGATCGAACCCTTGCGGCCGCCTACTAG TGGTGATGGTGGTGATGTGTGTAATCCTGGGGGTGTTGG C
LILRA3 HG13549-G (BioConnect)	Forward: CTCTAGAGGATCGAACCCTTGAATTCACCACCATGATGAC CTCCATCCTCACGGTC Reverse: CTAACCGGTAGGGATCGAACCCTTGCGGCCGCCTACTAG TGGTGATGGTGGTGATGCTCACCAGCCTTGGAGTCGGAC T

LILRA4 HG16058-G (BioConnect)	Forward: CTAACCGGTAGGGATCGAACCCTTGCGGCCGCCTACTAG TGGTGATGGTGGTGATGCTCACCAGCCTTGGAGTCGGAC T Reverse: CTAACCGGTAGGGATCGAACCCTTGCGGCCGCCTAGTGG TGATGGTGGTGATGATTCTCCACTGTGTAATCCTTGG
LILRA5 HG16059-G (BioConnect)	Forward: CTCTAGAGGATCGAACCCTTGGATCCACCACCATGGCAC CATGGTCTCATCCATC Reverse: CTAACCGGTAGGGATCGAACCCTTGCGGCCGCCTAGTGG TGATGGTGGTGATGGCGGATGAGATTCTCTACTGCG
LILRB2 HG14132-G (BioConnect)	Forward: CTCTAGAGGATCGAACCCTTGGATCCACCACCATGACCC CCATCGTCACAGTCCTG Reverse: CTAACCGGTAGGGATCGAACCCTTGCGGCCGCCTAGTGG TGATGGTGGTGATGCGACCCAGTGGGGGTGAGGGGC
LILRB4 HG16742-G (BioConnect)	Forward: CTCTAGAGGATCGAACCCTTGAATTCACCACCATGATCCC CACCTTCACGGCTCTG

	Reverse: CTAACCGGTAGGGATCGAACCCTTGCGGCCGCCTAGTGG TGATGGTGGTGATGCTCCCAGTCGGTTCTCAGACC
LILRB5 HG17221-G (BioConnect)	Forward: CTCTAGAGGATCGAACCCTTGGATCCACCACCATGACCCT CACCCTCTCAGTCCTG Reverse: CTAACCGGTAGGGATCGAACCCTTGCGGCCGCCTAGTGG TGATGGTGGTGATGCCCCAGGTGCCTTCCCAGACC

732

733

734 ## References

735 1. Dale DC, Boxer L, Liles WC. The phagocytes: neutrophils and monocytes. Blood.
736 2008;112(4):935–45. doi: 10.1182/blood-2007-12-077917.

737 2. Underhill DM, Rossnagle E, Lowell CA, Simmons RM. Dectin-1 activates Syk tyrosine
738 kinase in a dynamic subset of macrophages for reactive oxygen production. Blood.
739 2005;106(7):2543–50. doi: 10.1182/blood-2005-03-1239

740 3. Ravetch JV, Bolland S. IgG Fc receptors. Annu Rev Immunol. 2001;19:275–90. doi:
741 10.1146/annurev.immunol.19.1.275.

742 4. Huizinga TW, van Kemenade F, Koenderman L, Dolman KM, von dem Borne AE,
743 Tetteroo PA, et al. The 40-kDa Fc gamma receptor (FcRII) on human neutrophils is
744 essential for the IgG-induced respiratory burst and IgG-induced phagocytosis. J
745 Immunol. 1989;142(7):2365–9. doi: 10.4049/jimmunol.142.7.2365.

746 5. Lee WB, Kang JS, Yan JJ, Lee MS, Jeon BY, Cho SN, et al. Neutrophils Promote
747 Mycobacterial Trehalose Dimycolate-Induced Lung Inflammation via the Mincle
748 Pathway. PLoS Pathog. 2012;8(4):e1002614. doi: 10.1371/journal.ppat.1002614.

749 6. Brandsma AM, Hogarth PM, Nimmerjahn F, Leusen JHW. Clarifying the Confusion
750 between Cytokine and Fc Receptor “Common Gamma Chain”. Immunity.
751 2016;45(2):225–6. doi: 10.1016/j.immuni.2016.07.006.

752 7. Hirayasu K, Arase H. Functional and genetic diversity of leukocyte immunoglobulin-like
753 receptor and implication for disease associations. J Hum Genet. 2015;60(11):703–8.
754 doi: 10.1038/jhg.2015.64.

755 8. Mitchell A, Rentero C, Endoh Y, Hsu K, Gaus K, Geczy C, et al. LILRA5 is expressed by
756 synovial tissue macrophages in rheumatoid arthritis, selectively induces pro-
757 inflammatory cytokines and IL-10 and is regulated by TNF-alpha, IL-10 and IFN-gamma.

758 Eur J Immunol. 2008;38(12):3459–73. doi: 10.1002/eji.200838415.

759 9. Borges L, Kubin M, Kuhlman T. LIR9, an immunoglobulin-superfamily-activating
760 receptor, is expressed as a transmembrane and as a secreted molecule. Blood.
761 2003;101(4). doi: 10.1182/blood-2002-05-1432.

762 10. Lewis Marffy AL, McCarthy AJ. Leukocyte immunoglobulin-like receptors (LILRs) on
763 human neutrophils: Modulators of infection and immunity. Front Immunol. 2020;11:857.
764 doi: 10.3389/fimmu.2020.00857.

765 11. Burshtyn DN, Morcos C. The expanding spectrum of ligands for leukocyte Ig-like
766 receptors. J Immunol. 2016;196(3):947–55. doi: 10.4049/jimmunol.1501937.

767 12. Shang Y, Liu X, Wei L, Liang S, Zou Z, Wu M, et al. Leukocyte Immunoglobulin-like
768 Receptor A5 Deletion Aggravates the Pathogenesis of Pseudomonas aeruginosa
769 Keratitis by Promoting Proinflammatory Cytokines. Cornea. 2023;42(5):607–14. doi:
770 10.1097/ICO.0000000000003205.

771 13. Ning J, Fan X, Sun K, Wang X, Li H, Jia K, et al. Single-cell Sequence Analysis
772 Combined with Multiple Machine Learning to Identify Markers in Sepsis Patients:
773 LILRA5. Inflammation. 2023;46(4):1236–54. doi: 10.1007/s10753-023-01803-8.

774 14. Aleyd E, Heineke MH, van Egmond M. The era of the immunoglobulin A Fc receptor
775 FcαRI; its function and potential as target in disease. Immunol Rev. 2015;268(1):123–
776 38.

777 15. Zhao Y, van Woudenbergh E, Zhu J, Heck AJR, van Kessel KPM, de Haas CJC, et al.
778 The Orphan Immune Receptor LILRB3 Modulates Fc Receptor–Mediated Functions of
779 Neutrophils. J Immunol. 2020;204(4):954–66. doi: 10.4049/jimmunol.1900852.

780 16. Gao XM, Zhou XH, Jia MW, Wang XZ, Liu D. Identification of key genes in sepsis by
781 WGCNA. Prev Med. 2023;172:107540. doi: 10.1016/j.ypmed.2023.107540.

782 17. Demaret J, Venet F, Friggeri A, Cazalis MA, Plassais J, Jallades L, et al. Marked
783 alterations of neutrophil functions during sepsis-induced immunosuppression. J Leukoc
784 Biol. 2015;98(6):1081–90. doi: 10.1189/jlb.4A0415-168RR.

785 18. Dix A, Hünniger K, Weber M, Guthke R, Kurzai O, Linde J. Biomarker-based
786 classification of bacterial and fungal whole-blood infections in a genome-wide
787 expression study. Front Microbiol. 2015;6:171. doi: 10.3389/fmicb.2015.00171.

788 19. Herberg JA, Kaforou M, Wright VJ, Shailes H, Eleftherohorinou H, Hoggart CJ, et al.
789 Diagnostic Test Accuracy of a 2-Transcript Host RNA Signature for Discriminating
790 Bacterial vs Viral Infection in Febrile Children. JAMA. 2016;316(8):835–45. doi:
791 10.1001/jama.2016.11236.

792 20. Herwanto V, Tang B, Wang Y, Shojaei M, Nalos M, Shetty A, et al. Blood transcriptome
793 analysis of patients with uncomplicated bacterial infection and sepsis. BMC Res Notes.
794 2021 Feb 27;14(1):76. doi: 10.1186/s13104-021-05488-w.

795 21. Futosi K, Fodor S, Mócsai A. Neutrophil cell surface receptors and their intracellular
796 signal transduction pathways. Int Immunopharmacol. 2013 Nov;17(3):638–50. doi:
797 10.1016/j.intimp.2013.06.034.

798 22. Jones DC, Roghanian A, Brown DP, Chang C, Allen RL, Trowsdale J, et al. Alternative
799 mRNA splicing creates transcripts encoding soluble proteins from most LILR genes. Eur
800 J Immunol. 2009;39(11):3195–206. doi: 10.1002/eji.200839080.

801 23. Giraudi PJ, Pascut D, Banfi C, Ghilardi S, Tiribelli C, Bondesan A, et al. Serum
802 proteome signatures associated with liver steatosis in adolescents with obesity. J
803 Endocrinol Invest. 2024;48(1):213-225. doi: 10.1007/s40618-024-02419-x.

804 24. Fu YL, Harrison RE. Microbial Phagocytic Receptors and Their Potential Involvement in
805 Cytokine Induction in Macrophages. Front Immunol. 2021;12:662063. doi:
806 10.3389/fimmu.2021.662063.

807 25. Hirayasu K, Saito F, Suenaga T, Shida K, Arase N, Oikawa K, et al. Microbially cleaved
808 immunoglobulins are sensed by the innate immune receptor LILRA2. Nature Microbiol.
809 2016;1(6):16054. doi: 10/1038/nmicrobiol.2016.54.

810 26. van Sorge NM, Bonsor DA, Deng L, Lindahl E, Schmitt V, Lyndin M, et al. Bacterial
811 protein domains with a novel Ig-like fold target human CEACAM receptors. EMBO J.
812 2021;40(7):e106103. doi: 10.15252/embj.2020106103.

813 27. Köhler G, Milstein C. Continuous cultures of fused cells secreting antibody of predefined
814 specificity. Nature. 1975;256(5517):495–7. doi: 10.1038/256495a0.

815 28. Ohtsuka M, Arase H, Takeuchi A, Yamasaki S, Shiina R, Suenaga T, et al. NFAM1, an
816 immunoreceptor tyrosine-based activation motif-bearing molecule that regulates B cell
817 development and signaling. Proc Natl Acad Sci U S A. 2004;101(21):8126–31. doi:
818 10.1073/pnas.0401119101.

819 29. Scicluna BP, Uhel F, van Vught LA, Wiewel MA, Hoogendijk AJ, Baessman I, et al. The
820 leukocyte non-coding RNA landscape in critically ill patients with sepsis. Elife. 2020;9:
821 e58597. doi: 10.7554/eLife.58597.

822 30. Baghela A, Pena OM, Lee AH, Baquir B, Falsafi R, An A, et al. Predicting sepsis
823 severity at first clinical presentation: The role of endotypes and mechanistic signatures.
824 EBioMedicine. 2022;75:103776. doi: 10.1016/j.ebiom.2021.103776.

825 31. Hortová-Kohoutková M, De Zuani M, Lázničková P, Bendíčková K, Mrkva O,
826 Andrejčinová I, et al. Polymorphonuclear Cells Show Features of Dysfunctional
827 Activation During Fatal Sepsis. Front Immunol. 2021;12:741484. doi:
828 10.3389/fimmu.2021.741484.

829 32. Ahn SH, Tsalik EL, Cyr DD, Zhang Y, van Velkinburgh JC, Langley RJ, et al. Gene
830 expression-based classifiers identify Staphylococcus aureus infection in mice and
831 humans. PLoS One. 2013;8(1):e48979. doi: 10.1371/journal.pone.0048979.

832 33. Song R, Gao Y, Dozmorov I, Malladi V, Saha I, McDaniel MM, et al. IRF1 governs the
833 differential interferon-stimulated gene responses in human monocytes and
834 macrophages by regulating chromatin accessibility. Cell Rep. 2021;34(12):108891. doi:
835 10.1016/j.celrep.2021.108891.

836 34. Kleinertz H, Hepner-Schefczyk M, Ehnert S, Claus M, Halbgebauer R, Boller L, et al.
837 Circulating growth/differentiation factor 15 is associated with human CD56 natural killer
838 cell dysfunction and nosocomial infection in severe systemic inflammation.
839 EBioMedicine. 2019;43:380–91. doi: 10.1016/j.ebiom.2019.04.018.

840 35. Singer M, Deutschman CS, Seymour CW, Shankar-Hari M, Annane D, Bauer M, et al.
841 The Third International Consensus Definitions for Sepsis and Septic Shock (Sepsis-3).
842 JAMA. 2016;315(8). doi: 10.1001/jama.2024.0179.

843

844 Acknowledgements

845 We thank Birgit Maranca-Hüwel (University of Duisburg-Essen), Carla J.C. de Haas and Piet
846 Aerts (UMC Utrecht) for excellent technical support. We thank Bernhard B. Singer who passed
847 away in January 2023 for his involvement in the design and experimental part of this work.
848 This work was financed by the Biotechnology and Biological Sciences Research Council
849 (BBSRC, UK) grant BB/V006495/1 to A.J.M.; the Wellcome Trust grant 225315/Z/22/Z to
850 A.J.M.; by the European Union Horizon 2020 research and innovation programme under Grant
851 Agreement 700862; and the German research foundation grant 316213987/C06/B08 and
852 550453157 to N.L. and A.T.P; and the German Research Foundation Excellence Strategy
853 390713860 to M.B.

854

855 Conflict of interest

856 The authors declare no commercial or financial conflict of interest.

857 ## Author contributions

858 Z.F., M.R., I.K.-G., M.L., V.S., Y.Z., A.K. performed experiments. Z.F., M.R., I.K.-G., A.J.M
859 analysed data, visualised data, and wrote the original draft. N.L., A.T.P., S.B, S.B.F and G.W.
860 provided scientific help and critically reviewed the manuscript. A.J.M. I.K.-G. and B.B.S.
861 conceptualised and directed the study. A.J.M. supervised the analysis and interpretation of
862 the data. All authors contributed to the article and approved the submitted version.